

## Supporting Information

### **Films Morphology of Acrylonitrile Materials Deposited by Solution Process and Vacuum Evaporation. Supramolecular Interactions, Optoelectronic Properties and an Approximation by Computational Calculations.**

Enrique Pérez-Gutiérrez<sup>1</sup>, Margarita Cerón<sup>1</sup>, Pilar Santos<sup>1</sup>, Paulina Ceballos<sup>1</sup>, Venkatesan Perumal<sup>1</sup>, Subbiah Thamocharan<sup>2</sup>, Wilson Bernal-Pinilla<sup>3</sup>, Oracio Barbosa-García<sup>3</sup> and M. Judith Percino<sup>1\*</sup>.

<sup>1</sup>Unidad de Polímeros y Electrónica Orgánica, Instituto de Ciencias, Benemérita Universidad Autónoma de Puebla, Val3-Ecocampus Valsequillo, Independencia O2 Sur 50, San Pedro Zacachimalpa, Pue. México.

<sup>2</sup>Biomolecular Crystallography Laboratory, Department of Bioinformatics, School of Chemical and Biotechnology, SASTRA Deemed University, Thanjavur 613 401, India.

<sup>3</sup>Research Group of Optical Properties of Materials (GPOM), Centro de Investigaciones en Óptica A. P. 1-948, 37150 León Guanajuato, México.

Corresponding author:

M. Judith Percino;

judith.percino@correo.buap.mx

Unidad de Polímeros y Electrónica Orgánica,  
Benemérita Universidad Autónoma de Puebla,  
Val3-Ecocampus Valsequillo,  
Independencia O2 Sur 50,  
San Pedro Zacachimalpa, Pue., México.

## Lattice energy

The lattice energies of the compounds **A-D** were calculated by using the PIXEL program. Among three pyridyl scaffolds (2-pyridyl (**B**), 3-pyridyl (**C**) and 4-pyridyl (**D**)), the compound **D** has comparably higher lattice energy ( $-45.7 \text{ kcal mol}^{-1}$ ) and compound **C** having a lower lattice energy ( $-42.1 \text{ kcal mol}^{-1}$ ) than the other two. It is worthy to note that, all the three pyridyl scaffolds (**B-D**) have higher lattice energy than **A** ( $-40.4 \text{ kcal mol}^{-1}$ ), which is due to the phenyl instead of pyridyl moiety in the compound **A**. Interestingly, the dispersion energy component in all structures is predominant. The % electrostatic contribution (%  $E_{elec}$ ) is higher in **A** (22%) and its lower in **C** (18 %). It is to be noted that the Coulombic portion in **B** and **C** is slightly reduced when compared to **A** and **D** compounds.

Table S1. Lattice energies ( $\text{kcal mol}^{-1}$ ) partitioned into Coulombic, polarization, dispersion and repulsion contribution using CLP.

Dimer	Distance <sup>a</sup>	$E_{coul}$	$E_{pol}$	$E_{Disp}$	$E_{rep}$	$E_{tot}$	Symmetry	Important interactions	Geometry ( $\text{\AA}, \text{\circ}$ )			HS Label
									H...A	D...A	D-H...A	
<b>A</b>												
1	8.541	-3.0	-1.5	-14.9	8.0	-11.3	-x, 1-y, 1-z	C17-H17...Cg4	2.973	3.719	126	
								C18-H18...Cg4	3.270	3.857	115	
								C17-H17...C22	2.842	3.775	144	
2	8.842	-2.4	-1.5	-13.1	8.4	-8.7	-x, 2-y, 1-z	C26-H26...Cg3	2.674	3.540	136	
								C26-H26...H2-C2		2.364		
3	6.682	-4.8	-2.4	-7.7	7.6	-7.3	x, -1+y, z	C15-H15...N2	2.686	3.548	136	
								C19-H19...N2	2.240	3.283	160	
4	8.341	-1.6	-1.0	-8.1	4.3	-6.3	-x-1/2, y+1/2, -z+3/2	C10-H10...Cg3	2.976	3.654	121	2
								C11-H11...Cg3	2.802	3.802	111	
5	12.939	-1.8	-0.7	-7.0	3.5	-6.0	-x, 2-y, 2-z	C9-H9...Cg1	2.865	3.906	160	3
								C3-H3...C19	2.833	3.668	133	
6	10.452	-0.8	-0.6	-4.8	3.1	-3.1	-1/2+x, 3/2-y, -1/2+z	C3-H3...C20	2.794	3.757	147	
								C3-H3...C22	2.769	3.832	165	
7	15.906	-0.9	-0.3	-3.2	1.8	-2.6	-1/2-x, -1/2+y, 1/2-z	C24-H24...Cg4	3.026	3.904	138	
<b>B</b>												
1	5.926	-2.7	-1.1	-11.3	5.6	-9.5	1-x, -y, -z	C5-H5...N3	2.602	3.582	149	1
2	8.738	-2.8	-1.5	-11.3	7.6	-8.0	-1/2+x, 1/2-y, -1/2+z	C3-H3...N3	2.712	3.355	118	2
								C8-H8...Cg3	3.111	3.833	124	
3	9.947	-2.6	-1.2	-9.2	6.0	-7.0	-1/2+x, -1/2-y, -1/2+z	C19-H19...C3	2.743	3.783	160	3
								C24-H24...N2	2.727	3.692	148	
								C11-H11...C21	2.864	3.944	171	

									C25-H25...C16	2.754	3.532	128	4
									C25-H25...C19	2.861	3.882	156	
									C14-H14...C11	2.947	3.948	153	
4	9.127	-2.2	-1.6	-9.1	5.9	-6.9	-x, -y, -z		C15-H15...H10-C10		2.178		
5	9.881	-0.5	-0.5	-7.6	3.0	-5.7	1-x, -y, 1-z		C15-H15...C23	3.073	3.717	118	
6	8.160	-1.2	-1.1	-5.3	3.1	-4.6	1/2-x, 1/2+y, 1/2-z		C24-H24...C9	2.756	3.534	130.3	5
7	11.735	-2.2	-1.0	-6.0	5.3	-3.9	1/2-x, 1/2+y, -1/2-z		C4-H4...Cg2	2.435	3.480	160	6
8	10.188	-0.8	-0.4	-3.6	1.9	-2.9	3/2-x, -1/2+y, 1/2-z		C26-H26...Cg1	2.925	3.867	145	

**C**

									C11B-H11B...N2A	2.532	3.325	129	1
									C14B-H14B...Cg1A	2.774	3.730	146	2
									C6A-H6A...Cg1B	2.725	3.462	125	3
									C5B-H5B...C12A	2.730	3.389	119	4
2	7.666	-1.7	-1.4	-14.8	7.1	-10.9	1-x, y, 3/2-z		C2B-H2B...N3A	2.627	3.605	149	
									Cg4B...Cg3B		4.063		
									Cg4...Cgvinylic		3.639		
3	9.060	-2.6	-1.5	-16.3	10.6	-9.8	-x, y, 3/2-z		C25A-H25A...H12A-C12A		3.357		
									C8B-H8B...C10A	2.759	3.493	124	5
4	7.175	-2.5	-1.4	-13.5	8.8	-8.6	x, y, z		C8B-H8B...C9A	2.826	3.473	118	
									C18A-H18A...Cg2B	2.792	3.795	153	6
									C5B-H5B...N2A	2.572	3.391	131	7
									C15A-H15A...Cg1B	3.334	3.968	118	8
5	8.579	-2.9	-1.3	-11.1	7.2	-8.1	x, 1-y, 1/2+z		C26A-H26A...H9B-C9B		2.285		
									Cg4B...Cg4B		3.714		
6	13.173	-2.9	-1.2	-9.2	7.2	-6.0	1-x, y, 2-z		C5A-5A...C21B	2.954	3.982	158	
7	9.089	-0.5	-0.5	-6.8	2.6	-5.2	x, y, z-1/2		C4B-H4B...Cg3B	2.484	3.523	159	9
8	8.955	-1.7	-1.2	-7.2	5.6	-4.5	x, 2-y, z-1/2		C8A-H8A...C25B	2.751	3.442	121	10
9	13.219	-3.2	-1.7	-6.9	7.7	-4.2	1-x, y, 3/2-z		C24B-H224B...Cg1A	2.628	3.671	161	11
									C25A-H25A...N2A	2.729	3.382	118	
10	14.369	-1.2	-0.8	-7.7	5.9	-3.8	-x, y, 2-z		Cg4A...Cg4A		3.771		12
									C2A-H2A...H9A-C9A		2.336		
11	9.464	-1.2	-0.9	-6.0	4.5	-3.6	x, 1-y, z-1/2		C10A-H10A...Cg3A	2.640	3.627	150	13
									C25A-H25A...H6B-C6B		3.380		
12	114.15 3	-1.3	-0.7	-4.2	3.0	-3.2	-x, y, 3/2-z		C24A-H24A...Cg2B	2.721	3.809	178	14
13	12.844	-1.5	-0.5	-1.6	1.3	-2.3	1-x, -1+y, 3/2-z		C4A-H4A...N2B	2.587	3.489	140	15
14	14.734	-1.4	-0.5	-1.5	1.2	-2.2	1-x, 1-y, 2-z		C3A-H3A...N3B	2.627	3.709	172	

**D**

									C8-H8...Cg1	2.775	3.431	119	1
									C18-H18...Cg2	2.728	3.688	147	2
									C5-H5...C2	2.812	3.462	118	
									C2-H2...C25	2.670	3.637	148	3
2	8.041	-0.2	-1.3	-14.9	7.7	-8.8	1-x, y, 1/2-z		Cg3...Cg4		4.063		
3	13.436	-3.5	-1.1	-7.2	4.7	-7.91	1-x, 1-y, -z		Cg4...Cg4		3.838		
									C15-H15...C5	2.754	3.605	135	4
4	8.892	-1.1	-0.9	-8.9	5.0	-5.9	1/2-x, 1/2-y, -1/2+z		C9-H9...C21	2.792	3.820	157	
5	8.897	-1.8	-1.1	-7.2	5.1	-5.1	x, -y, 1/2+z		C4-H4...Cg3	2.590	3.603	154	5

									C4-H4...H12-C12	2.374		
									C5-H5...H12-C12	2.365		
6	12.894	-3.6	-1.4	-4.0	4.0	-5.1	1-x, -y, -z		C25-H25...N2	2.638	3.392	126
									C26-H26...N2	2.721	3.410	121
7	13.326	-2.0	-1.1	-5.3	4.2	-4.3	-1/2+x, -1/2+y, 1/2-z		C6-H6...N3	2.666	3.455	129
									C24-H24...Cg2	2.714	3.769	163
8	13.326	-1.4	-0.5	-1.8	1.6	-2.1	-1/2+x, 1/2+y, 1/2-z		C10-H10...N2	2.506	3.542	159

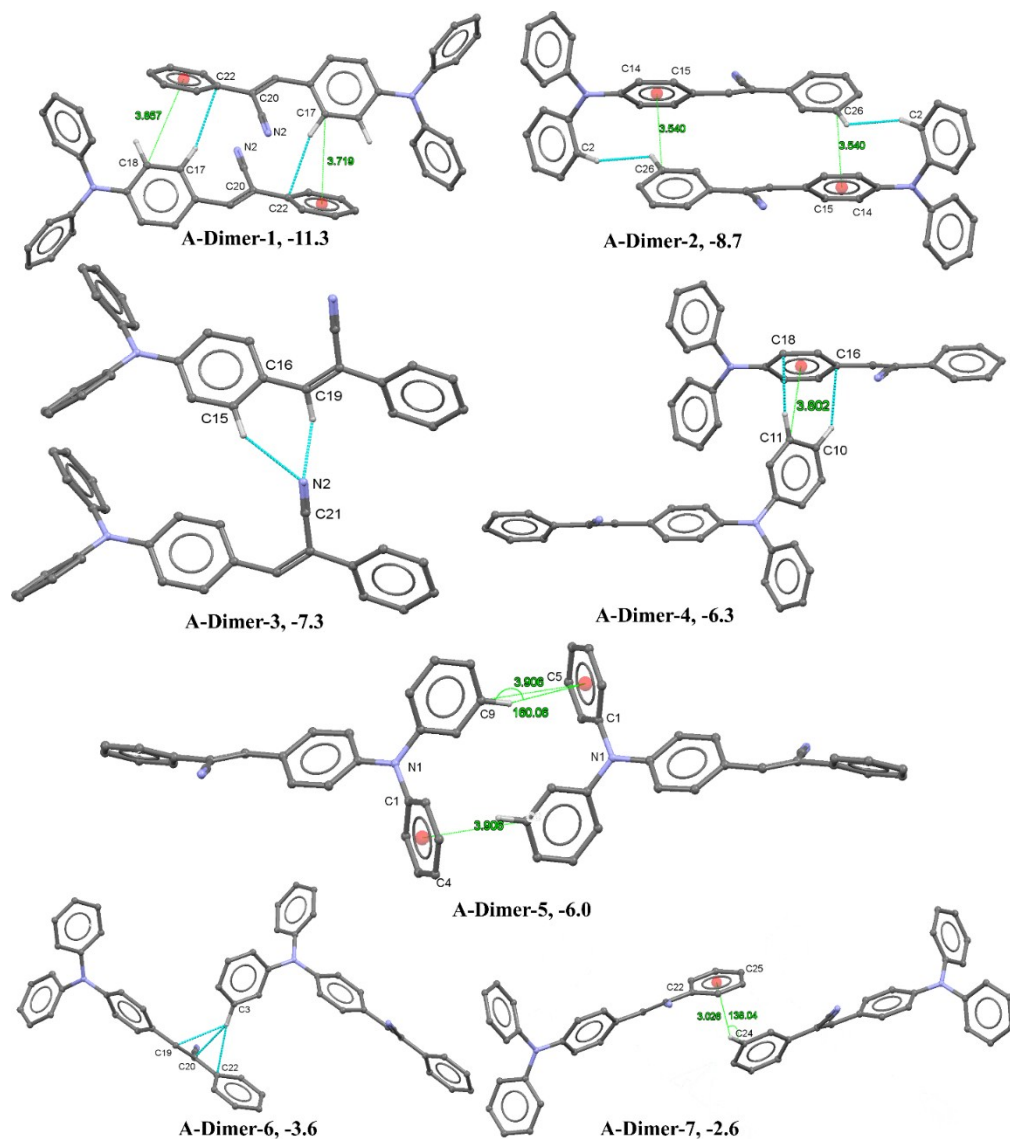


Figure S1. The energetically significant molecular dimers/pairs crystal packing of A along with interaction energies. ( $E_{tot}$  in kcal mol<sup>-1</sup>, refer Table SX).

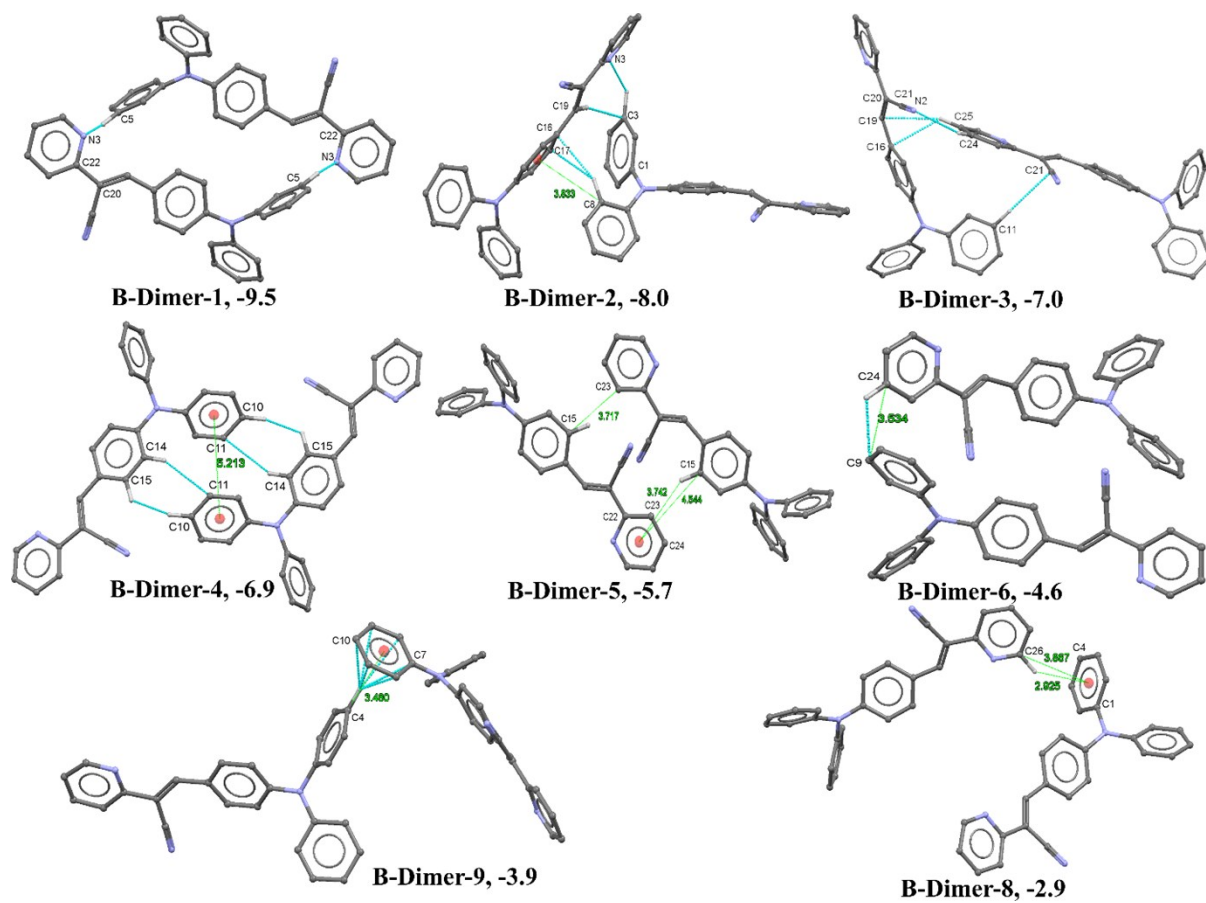


Figure S2. The energetically significant molecular dimers/pairs crystal packing of **B** along with interaction energies. ( $E_{tot}$  in kcal mol<sup>-1</sup>, refer Table S1).

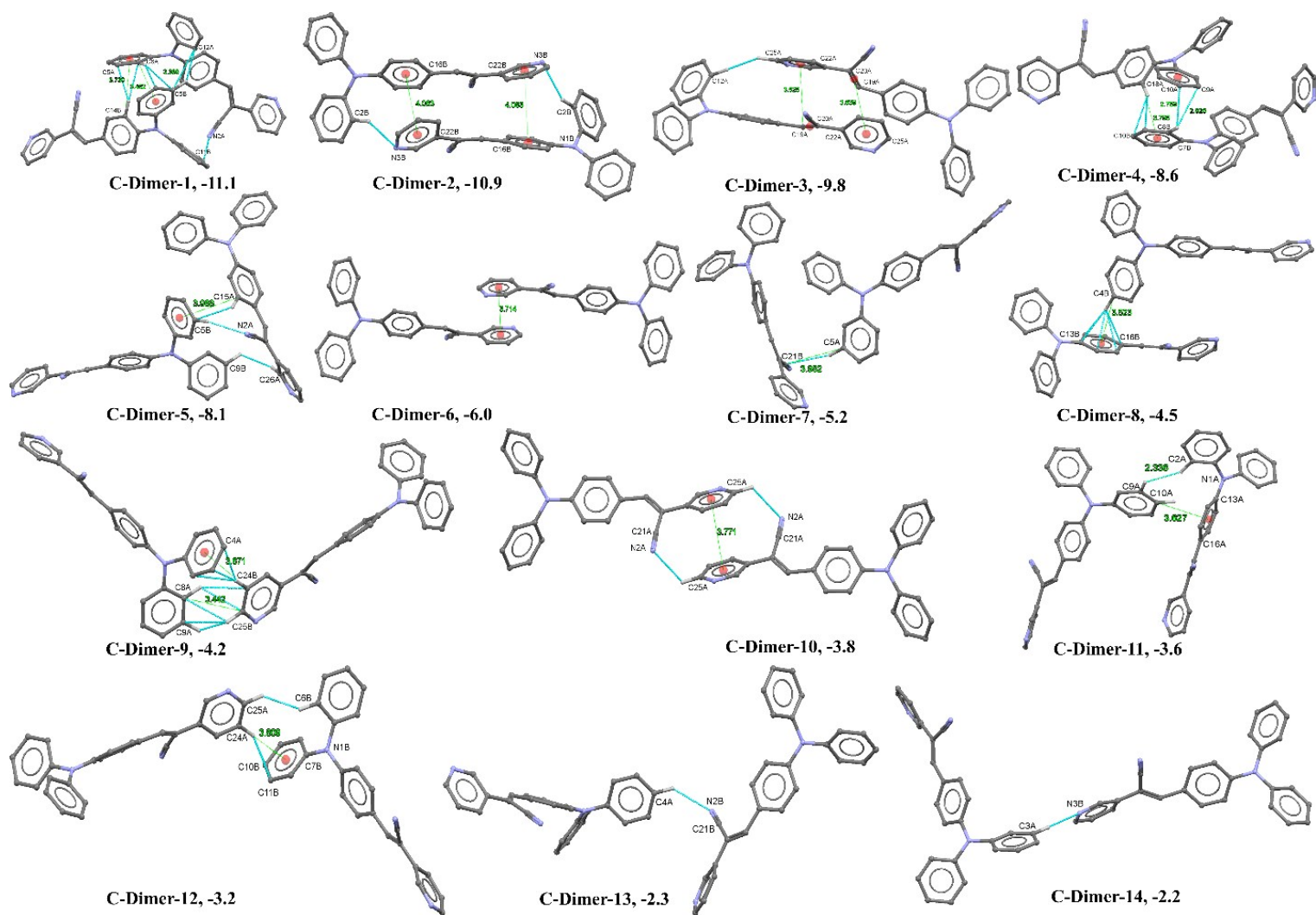


Figure S3. The energetically significant molecular dimers/pairs crystal packing of C along with interaction energies. ( $E_{tot}$  in kcal mol<sup>-1</sup>, refer Table S1).

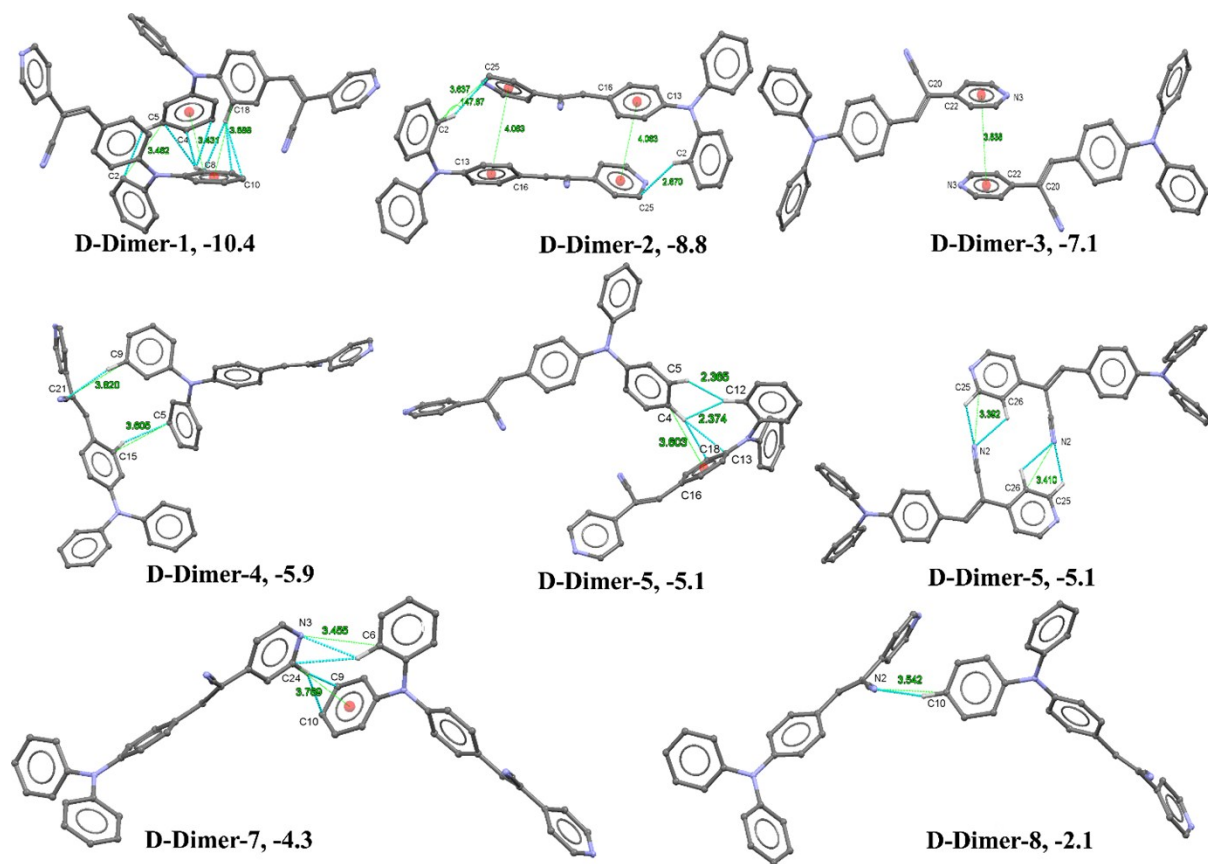


Figure S4. The energetically significant molecular dimers/pairs crystal packing of **D** along with interaction energies. ( $E_{tot}$  in kcal mol<sup>-1</sup>, refer Table S1).

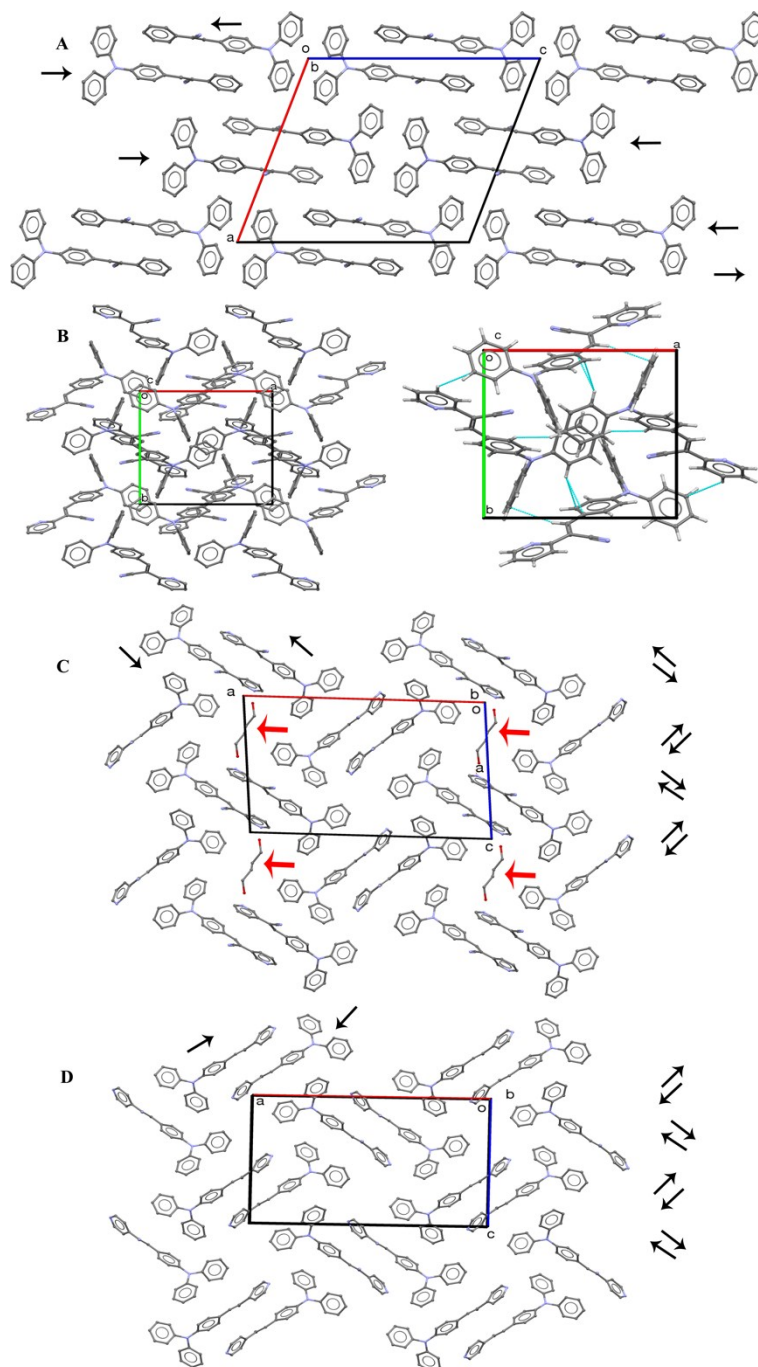


Figure S5. The packing diagram of **A-D**. (The solvent molecule in **C** is highlighted in red arrow)

In the crystalline state, the basic pattern observed in **A**, **C-D** as double arrays in a head (triphenylamine)-to-tail (phenyl/pyridine) fashion. The arrays are running in the anti-parallel direction in the double arrays (basic pattern) and the adjacent double arrays are arranged in parallel orientation in **A**. In contrast, arrays are arranged in the zig zag orientations and the



adjacent double arrays are arranged in parallel orientation in **C-D**. Interestingly, the disorder ethanol molecules in **C** are occupied in the cavity which was formed by the four dimeric unit. This disorder ethanol molecules are highlighted in Figure S5. There is no significant basic double array pattern was observed in **B** and the four molecules is forming a tetrameric structure as a basic pattern. This tetrameric structure is extended in all directions.

### Frontier molecular orbital analysis

From the frontier molecular orbitals (the highest occupied molecular orbitals (HOMO) and lowest unoccupied orbitals (LUMO)) in the gas phase of compounds **A-D** is shown in Figure S6. Generally, the electron density in HOMO's are mostly localized in the electron rich triphenyl amine moiety, whereas the electron in LUMO's are mostly localized in the electron poor pyridine and nitrile moiety. The HOMO values are found in the range of -5.650 – 5.767 eV and the LUMO values are in the range of -2.832 – 3.048 eV. From Figure S6, the HOMO-LUMO (band gap) values of compound **D** is slightly lower than the other compounds (**A-C**). This observation also supported that the compound **D** is the best conductor material than the other compound in the present study. Interestingly, the  $\Delta E_{(LUMO-HOMO)}$  value of compound **A** is comparably higher than the other pyridine scaffold (**B-D**) in the present study. From this observation, the  $N_{pyridine}$  atom in **B-D** significantly affected the energy level of respective orbitals.

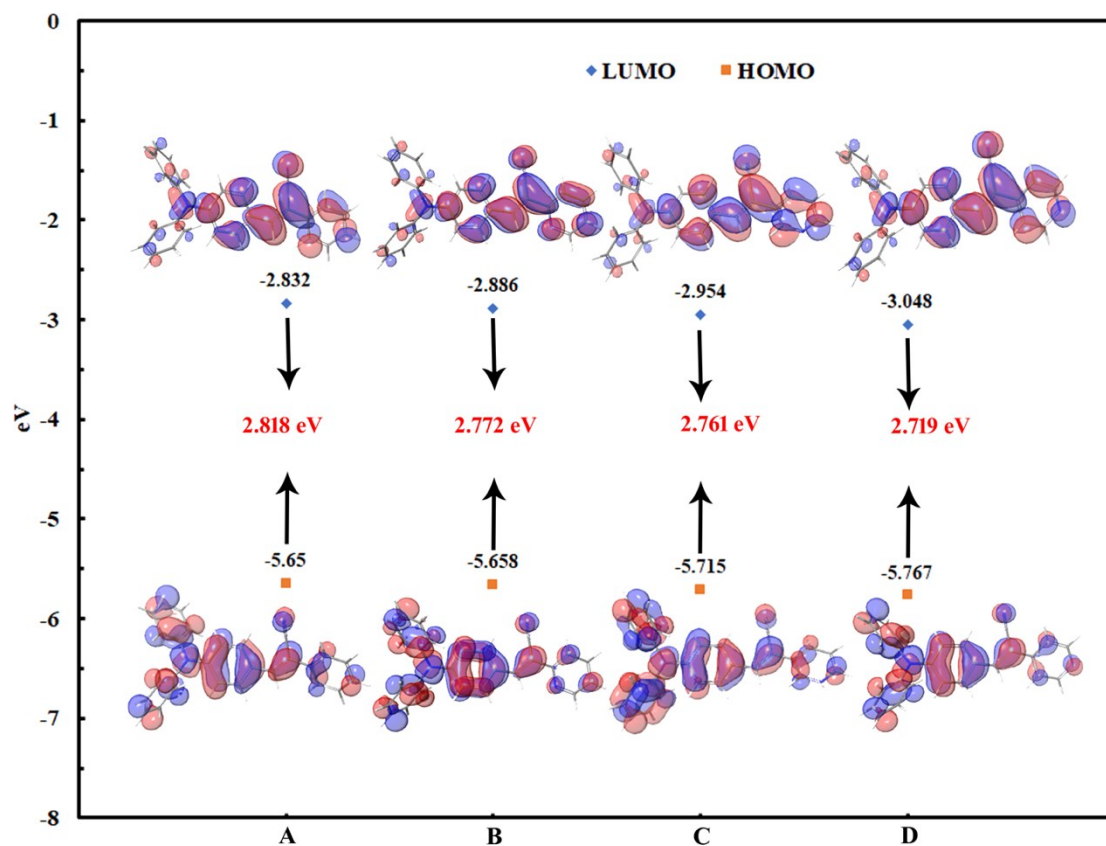


Figure S6. The HOMO-LUMO's diagrams of **A-D** along with the energy level. The red colour numerical value is represent for the  $\Delta E_{(LUMO-HOMO)}$ . (The B3LYP/MIDIX level of theory was used to compute the HOMO-LUMO's in gas phase. The corresponding orbitals are plotted with an isovalue=0.02  $\text{\AA}^{-3}$ ).